

# Scientific report - 2016 - project IDEI-0153: " ADVANCED STUDIES ON STRUCTURE AND DYNAMICS OF EXOTIC NUCLEI"

## I. Shape coexistence effects on isospin-related phenomena; terrestrial and stellar weak interaction rates for the $Z=N+2$ $^{70}\text{Kr}$ and $^{74}\text{Sr}$ nuclei

### I.1. Introduction

Proton-rich nuclei in the  $A\sim 70$  mass region are intensively investigated both theoretically and experimentally since their properties are relevant for the astrophysical rapid proton capture ( $rp$ ) process and could bring insights into fundamental symmetries and interactions. These nuclei manifest exotic nuclear structure and dynamics generated by the interplay between shape coexistence and mixing, competing like-nucleon and neutron-proton  $T=1$  and  $T=0$  pairing correlations, and isospin-symmetry-breaking interactions. Of particular importance could be the  $\beta$ -decay properties of the low-lying excited states of proton-rich nuclei situated on the  $rp$ -process path whose thermal population may influence their effective half-lives at the high temperatures of X-ray bursts [1]. Reliable predictions on the beyond experimental reach characteristics of these proton-rich nuclei require self-consistent microscopic description of the experimentally accessible properties. First we investigated the interplay between isospin-symmetry-breaking and shape-coexistence effects on the structure of  $A=70$  and  $A=74$  analogs within the *complex* Excited Vampir variational model [2]. Then we extended our investigations to the beta decay properties of the  $Z=N+2$  members of these isovector triplets in the frame of the *complex* Excited Vampir model using the same effective interaction and model space [3]. One of our aims is to realistically describe the strength distributions and half-life for  $^{70}\text{Kr}$  weak decay under terrestrial conditions and to present predictions on their characteristic behaviour in the X-ray burst astrophysical environment. The present study is the first attempt at a completely self-consistent calculation of the terrestrial and stellar weak interaction rates for  $^{70}\text{Kr}$  at densities  $\rho = 10^4 - 10^7 g/cm^3$  and temperatures  $T = 10^8 - 10^{10} K$  using the *complex* Excited Vampir approach.

Investigations based on the variational approaches of the VAMPIR model family have been successfully performed for coexistence phenomena manifested by proton-rich nuclei in the  $A\sim 70$  mass region, in particular, on exotic structure as well as allowed Fermi (F) and Gamow-Teller (GT)  $\beta$ -decay properties of nuclei close to the  $N=Z$  line [2-7]. The *complex* Excited Vampir approach allows for a unified description of structure and dynamics at low- and high-spins including in the symmetry projected mean fields neutron-proton pairing correlations in both  $T=1$  and  $T=0$  channels and general two-nucleon unnatural-parity correlations. The beyond-mean-field *complex* Ex-

cited Vampir model allows to realistically describe the characteristic features of nuclei in the  $A\sim 70$  mass region like shape coexistence and mixing and the strong variation of the deformation with number of nucleons, increasing spin, and excitation energy. The Vampir results nicely compare to the available experimental information and many predictions are confirmed by the data. Since the Vampir approaches enable the use of rather large model spaces and of general two-body interactions, *large-scale* nuclear structure studies going far beyond the abilities of the conventional shell-model configuration-mixing approach are possible. Our previous investigations on coexistence phenomena in  $N\approx Z$  nuclei in this mass region indicated for a given symmetry the presence of a variable sometimes strong mixing of differently deformed configurations in the intrinsic system. Furthermore, as expected, beside the like-nucleon pairing the neutron-proton pairing correlations were found to play an important role ([2] and references therein).

### I.2. Theoretical Framework

The *complex* Excited Vampir (EXVAM) approach uses the most general Hartree-Fock-Bogoliubov (HFB) vacua as basic building blocks being only restricted by time-reversal and axial symmetry. The underlying HFB transformations are essentially *complex* and do mix proton-with neutron-states as well as states of different parity and angular momentum. The HFB vacua of this type account for arbitrary two-nucleon correlations and thus simultaneously describe like-nucleon as well as isovector and isoscalar neutron-proton pairing correlations. The broken symmetries of these vacua (nucleon numbers, parity, total angular momentum) are restored by projection before variation and the resulting symmetry-projected configurations are then used as test wave functions. Chains of successive variational calculations are accomplished independently for each spin and parity to determine the underlying HFB transformations. First the Vampir solutions, representing the optimal mean-field description of the yrast states by single symmetry-projected HFB determinants are obtained. Then the Excited Vampir approach is used to construct additional excited states by independent variational calculations. The final solutions for each considered symmetry are obtained diagonalizing the residual interaction between the successively constructed orthogonal many-nucleon Excited Vampir configurations.

For nuclei in the  $A \sim 70$  mass region we use a  $^{40}\text{Ca}$  core and include the  $1p_{1/2}$ ,  $1p_{3/2}$ ,  $0f_{5/2}$ ,  $0f_{7/2}$ ,  $1d_{5/2}$  and  $0g_{9/2}$  oscillator orbits for both protons and neutrons in the valence space. We start with an isospin symmetric basis and then introduce the Coulomb shifts for the proton single-particle levels resulting from the  $^{40}\text{Ca}$  core by performing spherically symmetric Hartree-Fock calculations using the Gogny-interaction D1S in a 21 major-shell basis [2]. The effective two-body interaction is constructed from a nuclear matter G-matrix based on the charge-dependent Bonn CD potential. In order to enhance the pairing correlations this G-matrix was modified by adding short-range (0.707 fm) Gaussians with strength of -35 MeV in the T=1 proton-proton and neutron-neutron channel, -20 MeV in the neutron-proton T=1 channel, and -35 MeV in the neutron-proton T=0 channel. In addition, the isoscalar interaction was modified by monopole shifts for all T=0 matrix elements of the form  $\langle 1p1d_{5/2}; IT = 0 | \hat{G} | 1p1d_{5/2}; IT = 0 \rangle$ , where 1p denotes either the  $1p_{1/2}$  or the  $1p_{3/2}$  orbit, and  $\langle 0g_{9/2}0f; IT = 0 | \hat{G} | 0g_{9/2}0f; IT = 0 \rangle$ , where 0f denotes either the  $0f_{5/2}$  or the  $0f_{7/2}$  orbitals [2]. These monopole shifts have been introduced in our earlier calculations in order to influence the onset of deformation. Previous results indicated that the oblate-prolate coexistence and mixing at low spins sensitively depend on the strengths of the neutron-proton T=0 matrix elements involving nucleons occupying the  $0f_{5/2}$  or  $0f_{7/2}$  and  $0g_{9/2}$  single particle orbits. The Hamiltonian includes the two-body matrix elements of the Coulomb interaction between the valence protons.

### I.3. Results and Discussion

We investigated the isospin-symmetry-breaking effects taking into account both the Coulomb interaction and the isospin-symmetry violation by the strong force as it is considered by the Bonn CD potential. We obtained results on the effect of isospin mixing on Coulomb energy differences (CED), mirror energy differences (MED), triplet energy differences (TED), and triplet displacement energy (TDE) in the  $A=70$  and  $A=74$  isovector triplets studying the  $0^+$ ,  $2^+$ ,  $4^+$ , and  $6^+$  states in these nuclei. Figure 1 illustrates the complex Excited Vampir predictions on mirror energy differences and triplet energy differences for the  $A = 74$  isovector triplet. MED manifest a positive trend, while TED indicate a negative trend, in agreement with the recent experimental available results [2].

For the investigation of the Fermi and Gamow-Teller  $\beta$ -decay properties of the lowest two  $0^+$  and  $2^+$  states in  $^{70}\text{Kr}$  we extended the calculations presented in [2] to the daughter states in the  $^{70}\text{Br}$  nucleus. We constructed up to 80 many-nucleon *complex* Excited Vampir configurations for the spin  $1^+$  and  $3^+$  in  $^{70}\text{Br}$  [3]. The structure of the even-spin yrast states in both, parent  $^{70}\text{Kr}$  and daughter nucleus  $^{70}\text{Br}$ , are discussed in [2]. In  $^{70}\text{Kr}$  the wave functions of the ground state and yrast  $2^+$  state

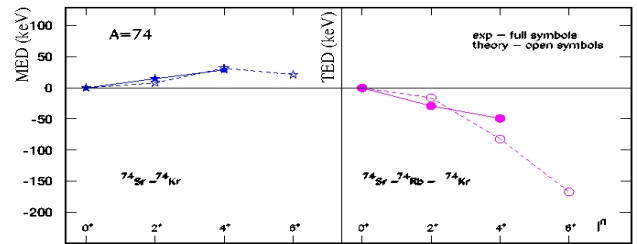


FIG. 1. The *complex* Excited VAMPIR results for MED and TED in the  $A=74$  isovector triplet compared to data [2].

are dominated by prolate components (almost 73%), the first excited  $0^+$  indicates almost equal prolate (48%) and oblate (52%) content, while the second  $2^+$  state is dominated by oblate configurations in the intrinsic system (almost 73%). Strong, similar oblate-prolate mixing was found in the lowest  $0^+$  and  $2^+$  states in  $^{70}\text{Br}$ , for both spins obtaining almost 70% prolate (oblate) content in the lowest (first excited) state. As we may expect variable, for some states very strong, mixing of differently deformed prolate and oblate configurations in the intrinsic system was found in the structure of the wave functions for the daughter  $1^+$  and  $3^+$  states in  $^{70}\text{Br}$ . The large variety of shape mixing in the structure of the states populated by Gamow-Teller  $\beta$ -decay of  $^{70}\text{Kr}$  is reflected by the spectroscopic quadrupole moments of the corresponding states in Figs. 2, 3. Significant difference is found in the energy interval between the lowest two  $0^+$  and  $2^+$  states in  $^{70}\text{Kr}$ . In  $^{70}\text{Kr}$  the lowest two  $0^+$  ( $2^+$ ) states are separated by 1.718 (0.982) MeV.

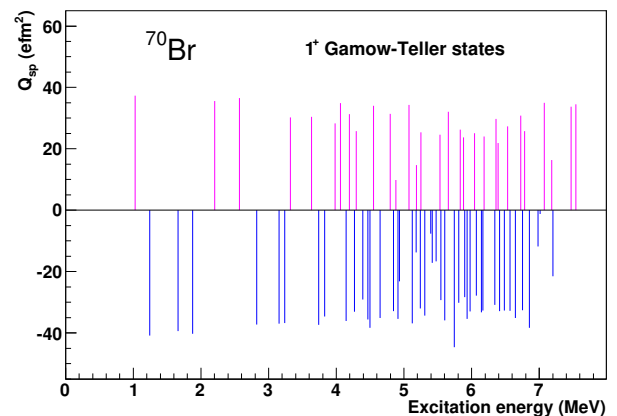


FIG. 2. Spectroscopic quadrupole moments for daughter  $1^+$  states in  $^{70}\text{Br}$ .

We illustrate the *complex* Excited Vampir results on the Fermi strength distributions by the decay of the yrast  $2^+$  state in  $^{70}\text{Kr}$  presented in Fig. 4. Concerning the Gamow-Teller strength distributions it is worthwhile to mention that the strongest branches in the decay of the

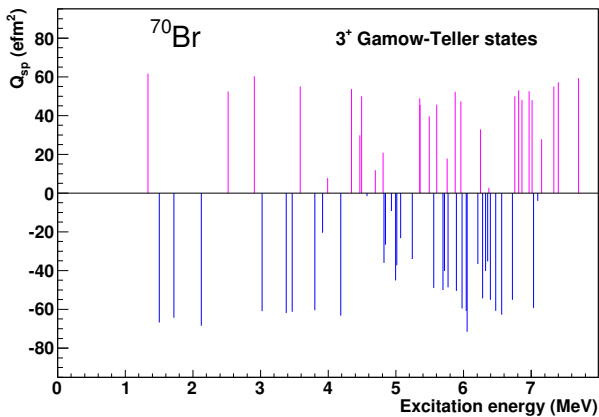


FIG. 3. The same as in Fig. 2, but for  $3^+$  states.

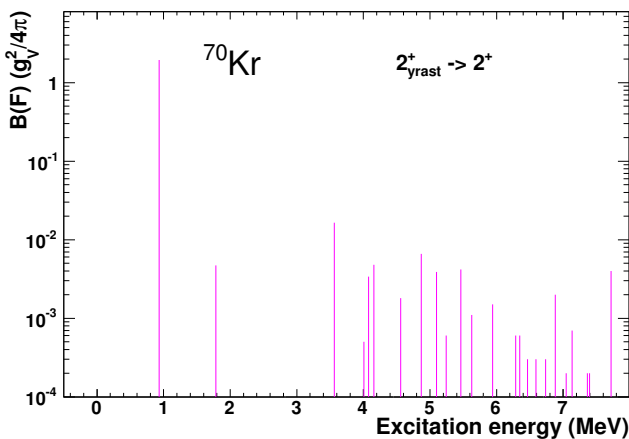


FIG. 4. Fermi strength distribution for the decay of the yrast  $2^+$  in  $^{70}\text{Kr}$  to  $2^+$  states in  $^{70}\text{Br}$  obtained within the *complex Excited Vampir* model.

ground state are feeding  $1^+$  states in the daughter nucleus showing spectroscopic quadrupole moments of different sign (the second and the fifth  $1^+$  with increasing excitation energy in Fig.2). The analysis of the structure of the GT branches to the lowest five  $1^+$  states indicates that strong branches are built out either from a coherent contribution of  $p_{1/2}^{\nu(\pi)} p_{3/2}^{\pi(\nu)}$ ,  $p_{3/2}^{\nu} p_{3/2}^{\pi}$ ,  $f_{5/2}^{\nu} f_{5/2}^{\pi}$ ,  $f_{5/2}^{\nu(\pi)} f_{7/2}^{\pi(\nu)}$ , and  $g_{9/2}^{\nu} g_{9/2}^{\pi}$  matrix elements or from a strong contribution of  $g_{9/2}^{\nu} g_{9/2}^{\pi}$  ones, while weak GT branches show cancellation of all these contributing matrix elements. In Fig. 5 and Fig. 6 we present the GT strength distributions for the decay of the yrast  $2^+$  in  $^{70}\text{Kr}$ . The analysis of the GT strength distributions for the decay of the yrast  $2^+$  to the  $1^+$  states in  $^{70}\text{Br}$  indicates similar behaviour with the GT decay of the ground state, but much weaker branches, while stronger branches are revealed by the strength distribution to the  $3^+$  states. Very weak transi-

tion strengths have been found for the decay of the yrast  $2^+$  state in  $^{70}\text{Kr}$  to  $2^+$  states in  $^{70}\text{Br}$ .

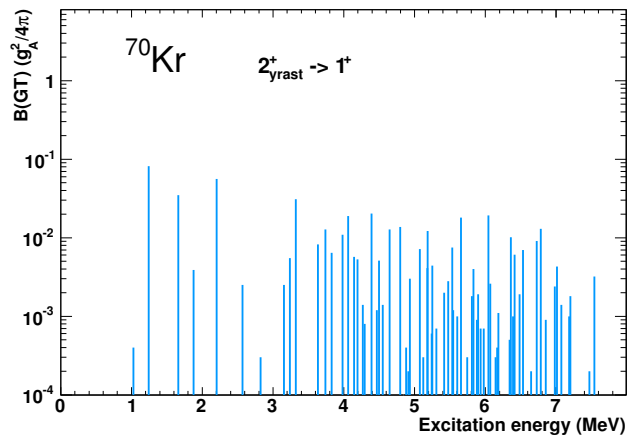


FIG. 5. Gamow-Teller strength distribution for the decay of the yrast  $2^+$  in  $^{70}\text{Kr}$  to  $1^+$  states in  $^{70}\text{Br}$ .

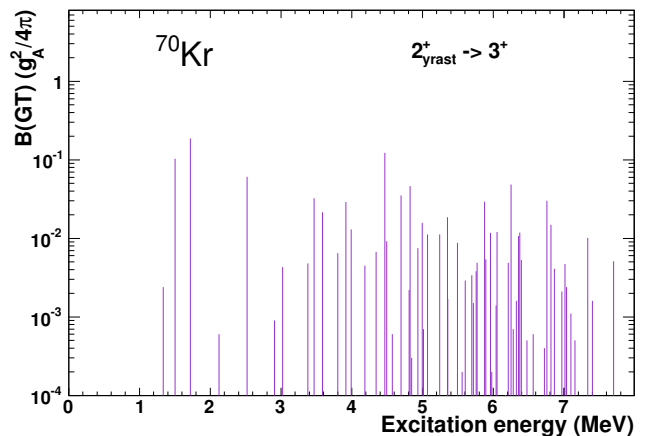


FIG. 6. The same as in Fig. 5, but for the decay to  $3^+$  states in  $^{70}\text{Br}$ .

The GT accumulated strengths presented in Fig. 7 for the decay of the ground state, first excited  $0^+$ , and yrast  $2^+$  state in  $^{70}\text{Kr}$  to the daughter states in  $^{70}\text{Br}$  indicate stronger strength from the ground state decay with respect to that from the first excited  $0^+$  state and larger contributions from the decay of the yrast  $2^+$  state to the daughter  $3^+$  states than the ones to the  $1^+$  states. In order to evaluate the half-life under terrestrial conditions as well as in the X-ray burst environment we studied the effect of the isospin mixing on the superallowed Fermi  $\beta$ -decay of the ground state and yrast  $2^+$  state in  $^{70}\text{Kr}$  to the analog states in  $^{70}\text{Br}$ . We calculated the half-life of  $^{70}\text{Kr}$  using beta window  $Q_{EC} = 10.480$  MeV. The terrestrial F and GT half-life for the decay of the ground

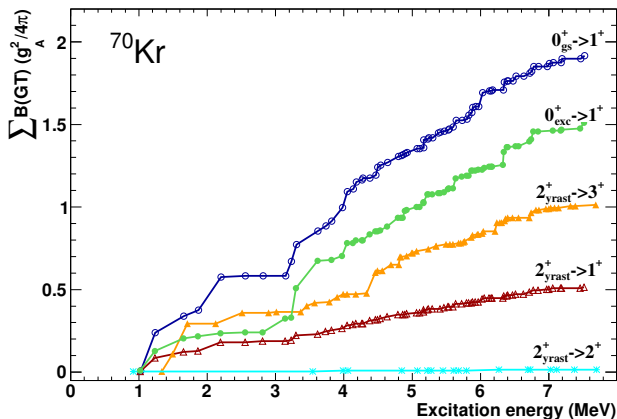


FIG. 7. Gamow-Teller accumulated strengths for the decay of the ground state, first excited  $0^+$ , and yrast  $2^+$  state in  $^{70}\text{Kr}$  to the daughter states in  $^{70}\text{Br}$  obtained within *complex* Excited Vampir model.

state of  $^{70}\text{Kr}$  is obtained by

$$\frac{1}{T_{1/2}} = \frac{1}{K} \sum_{E_f} f(Z, E_f) [B_{if}(F) + B_{if}(GT)], \quad (1)$$

where  $E_f$  denotes the energy of the final state,  $K=6146$  s and  $f(Z, E_f)$  are the Fermi integrals. The Fermi and Gamow-Teller reduced transition probabilities can be written as

$$B_{if}(F) = \frac{1}{2J_i + 1} |M_F|^2, \quad (2)$$

$$B_{if}(GT) = \frac{1}{2J_i + 1} \left( \frac{g_A}{g_V} \right)^2 |M_{GT}|^2, \quad (3)$$

where  $g_A/g_V = -1.26$ . The Fermi and Gamow-Teller nuclear matrix elements between the initial ( $|\xi_i J_i \rangle$ ) and the final ( $|\xi_f J_f \rangle$ ) states of spin  $J_i$  and  $J_f$ , respectively,

$$\begin{aligned} M_F &\equiv (\xi_f J_f | \hat{1} | \xi_i J_i) \\ &= \delta_{J_i J_f} \sum_{ab} M_F(ab) (\xi_f J_f | [c_a^\dagger \tilde{c}_b]_0 | \xi_i J_i), \end{aligned} \quad (4)$$

$$\begin{aligned} M_{GT} &\equiv (\xi_f J_f | \hat{\sigma} | \xi_i J_i) \\ &= \sum_{ab} M_{GT}(ab) (\xi_f J_f | [c_a^\dagger \tilde{c}_b]_1 | \xi_i J_i), \end{aligned} \quad (5)$$

are composed of the reduced single-particle matrix elements of the unit operator  $\hat{1}$ ,  $M_F(ab) = (a | \hat{1} | b)$ , and Pauli spin operator  $\sigma$ ,  $M_{GT}(ab) = \frac{1}{\sqrt{3}} (a | \hat{\sigma} | b)$ , and the reduced one-body transition densities calculated using

the harmonic oscillator wave functions [3]. For the  $\beta^+$ -decay and electron capture,  $c_a^\dagger$  is the neutron creation operator and  $\tilde{c}_b$  is the proton annihilation operator and the sum runs over the valence nucleons.

The *complex* Excited Vampir result for the Gamow-Teller half-life of the ground state of  $^{70}\text{Kr}$  is 258 ms and for the Fermi decay is 63 ms. Consequently, the theoretical half-life of the ground state amounts to 51 ms in good agreement with the available experimental values of 57(21) ms, 42(31) ms, adopted 52(17) ms, and the most recent preliminary value of 40(6) ms. The agreement between the *complex* Excited Vampir results for the terrestrial decay and the available data on half-life gives support to our predictions on the  $\beta$ -decay strength distributions for the low-lying excited states in  $^{70}\text{Kr}$  isotope. Using the present predictions as well as our previous results [2] concerning the excitation energy of these states we shall present in the following the *complex* Excited Vampir results on the stellar weak interaction rates for the investigated  $Z=N+2$  nuclei in the X-ray burst environment.

The general formalism to calculate weak interaction rates for a stellar environment has been introduced by Fuller et al. [8]. Relevant for the astrophysical scenarios of explosive phenomena are the properties of exotic nuclei difficult to investigate experimentally or beyond the experimental reach. Previous studies suggested that in the ranges of densities and temperatures relevant for the *rp* process the stellar beta decay and continuum electron capture characteristics are sensitive to the strength distributions. Consequently, a realistic description of the shape coexistence and mixing dominating the structure of the low-lying states of  $A \sim 70$  proton-rich nuclei and the corresponding daughter states is required.

The procedure used to obtain the weak interaction decay rates in the stellar environment is presented in [2].

For the  $Z=N+2$  nucleus  $^{70}\text{Kr}$  we investigated the influence of the yrast  $2^+$  state decay on the effective half-life given the predicted high excitation energy of the first excited  $0^+$  and the second  $2^+$  states. The Gamow-Teller  $\beta$ -decay rates as a function of temperature decomposed into contributions from the ground state of  $^{70}\text{Kr}$  to the daughter  $1^+$ ,  $2^+$ , and  $3^+$  are depicted in Fig. 8. The influence of the decay of the  $2^+$  state on the total decay rate appears only at temperatures  $T > 2.5\text{GK}$ . In Fig. 9 the Fermi and Gamow-Teller  $\beta^+$ -decay (left) and continuum electron capture rates for *rp*-process peak density  $\rho Y_e = 10^6$  ( $\text{mol}/\text{cm}^3$ ) (right) are decomposed into the contributions from the ground state and yrast  $2^+$  state of  $^{70}\text{Kr}$  to the daughter states in  $^{70}\text{Br}$ . As it is illustrated in Fig. 10 (left) the contribution of the electron capture is very small at the temperatures (1 – 3GK) and densities ( $10^6 - 10^7 \text{g}/\text{cm}^3$ ) characteristic for the *rp*-process astrophysical environment. Our previous investigations on the stellar weak interaction rates for the waiting point nuclei  $^{68}\text{Se}$  and  $^{72}\text{Kr}$  revealed a very strong contribution from the continuum electron capture at the *rp*-process

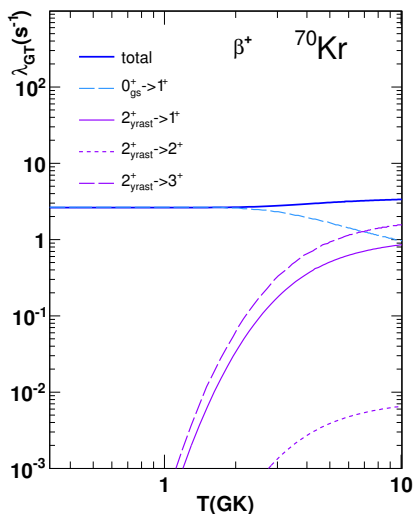


FIG. 8. Gamow-Teller  $\beta$ -decay rates ( $s^{-1}$ ) for the ground state and yrast  $2^+$  state of  $^{70}\text{Kr}$  as a function of temperature  $T$  (GK) obtained within *complex* Excited Vampir model.

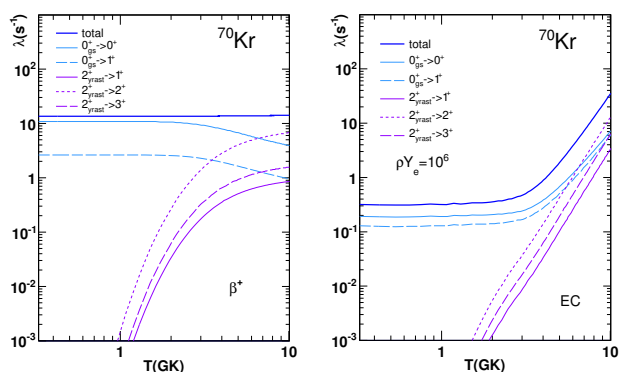


FIG. 9. Fermi and Gamow-Teller decay rates ( $s^{-1}$ ) of  $^{70}\text{Kr}$  for  $\beta^+$  (left) and continuum electron capture for  $rp$ -process peak density  $\rho Y_e = 10^6$  ( $\text{mol}/\text{cm}^3$ ) (right) as a function of temperature  $T$  (GK).

peak conditions [6]. The total decay rates for  $^{70}\text{Kr}$  at the  $rp$ -process peak density as a function of temperature are presented in Fig. 10 (right) decomposed into the contributions from the ground state and yrast  $2^+$  state. Extended investigations have been accomplished for the  $Z=N+2$   $^{74}\text{Sr}$  nucleus (Fig.11) [3].

Finally, in Fig. 12 are presented the half-lives for  $^{70}\text{Kr}$  for two selected densities  $\rho Y_e$  as a function of temperature. The results indicate that under  $rp$ -process typical conditions the effective half-lives are not changed with respect to the values found under terrestrial conditions. The present report represent the first beyond-mean-field treatment based on an effective two-body interaction con-

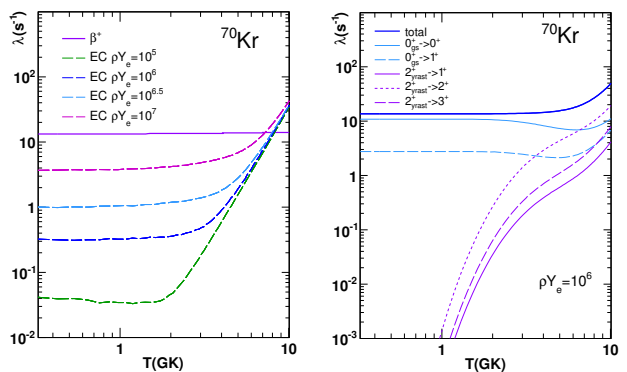


FIG. 10. Fermi and Gamow-Teller decay rates ( $s^{-1}$ ) for the ground state and yrast  $2^+$  state of  $^{70}\text{Kr}$  decomposed into the corresponding  $\beta^+$  and electron capture components for selected densities  $\rho Y_e$  ( $\text{mol}/\text{cm}^3$ ) (left) and total decay rates for  $rp$ -process peak density (right) as a function of temperature  $T$  (GK). [3]

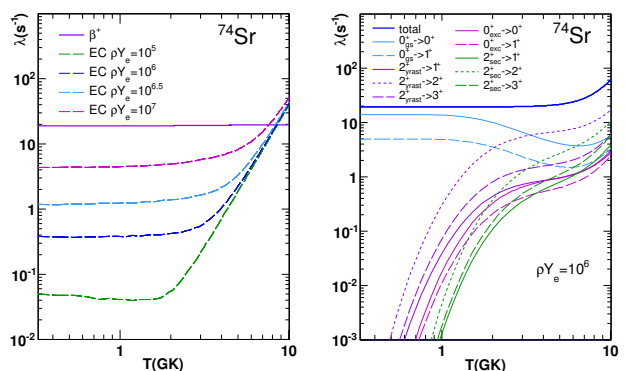


FIG. 11. The same as in Fig. 10, but for  $^{74}\text{Sr}$  nucleus [3].

structed from the nuclear matter G-matrix starting from the charge dependent Bonn CD potential able to describe self-consistently the allowed Fermi and Gamow-Teller  $\beta$ -decay [3, 7] as well as the effect of shape coexistence on isospin-related phenomena in the corresponding isovector triplets [2, 5] in a region dominated by shape coexistence and mixing. Furthermore, we use a model space adequate for the description of proton-rich nuclei in the  $A \sim 70$  mass region which is not yet numerically feasible for the large-scale shell-model calculations. Experimental strength distributions and spectroscopic quadrupole moments for the parent and daughter states could test our predictions on the influence of shape mixing on weak interaction rates.

#### I. 4. Conclusions

In this report we present the first self-consistent results on the effect of shape mixing on isospin-related phenom-

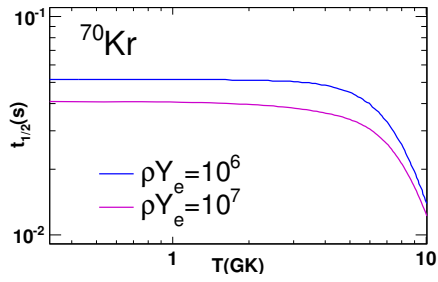


FIG. 12. Half-lives ( $s$ ) for  $^{70}\text{Kr}$  for selected densities  $\rho Y_e$  ( $\text{mol}/\text{cm}^3$ ) as a function of temperature  $T$  (GK).

ena in proton-rich  $A \sim 70$  nuclei and on the terrestrial and stellar weak interaction rates for the  $Z=N+2$   $^{70}\text{Kr}$  and  $^{74}\text{Sr}$  isotopes describing the low-lying  $0^+$  and  $2^+$  states in the parent nuclei and the corresponding daughter  $0^+$ ,  $1^+$ ,  $2^+$ , and  $3^+$  states in  $^{70}\text{Br}$  and  $^{74}\text{Rb}$ , respectively, within the *complex* Excited Vampir model based on an effective interaction obtained from the charge-dependent Bonn CD potential and an appropriate model space. Of course, experimental information is needed on the strength distributions for the  $^{70}\text{Kr}$  and  $^{74}\text{Sr}$  decay to confirm our predictions.

- 
- [1] H. Schatz *et al.*, Phys. Rep. **294**, 167 (1998).  
 [2] A. Petrovici, Phys. Rev. C **91**, 014302 (2015).  
 [3] A. Petrovici and O. Andrei, Phys. Rev. C **92**, 064305 (2015).  
 [4] A. Petrovici, Rom. J. Phys. **58**, 1120 (2013).  
 [5] A. Petrovici, J. Phys. Conf. Ser. **724**, 012038 (2016).  
 [6] A. Petrovici and O. Andrei, Eur. Phys. J. A **51**, 133 (2015).  
 [7] A. Petrovici and O. Andrei, will appear in AIP Conf. Proc. (2016).  
 [8] G. M. Fuller, W. A. Fowler, M.J. Newman, Astrophys. J. Suppl. Ser. **42**, 447 (1980).

## II. Structure of yrast states in $^{100}\text{Ru}$ within *complex* Excited Vampir model

### II. 1. Introduction

The structure of neutron-rich nuclei in the  $A \simeq 100$  mass region manifests drastic changes in some isotopic chains and often sudden variations of particular nuclear properties have been identified. Neutron-rich Sr and Zr nuclei indicate rapid transition from spherical to deformed shape with a possible identification of triple shape coexistence in the  $N=58$   $^{96}\text{Sr}$  and  $^{98}\text{Zr}$  [1]. We studied the evolution in structure with increasing spin in  $^{100}\text{Ru}$  within the *complex* Excited Vampir (EXVAM) variational model with symmetry projection before variation using a realistic effective interaction based on Bonn CD potential in a large model space [2].

### II. 2. Theoretical Framework

For nuclei in the  $A \simeq 100$  mass region is used a rather large model space above the  $^{40}\text{Ca}$  core built out of  $1p_{1/2}$ ,  $1p_{3/2}$ ,  $0f_{5/2}$ ,  $0f_{7/2}$ ,  $2s_{1/2}$ ,  $1d_{3/2}$ ,  $1d_{5/2}$ ,  $0g_{7/2}$ ,  $0g_{9/2}$ , and  $0h_{11/2}$  oscillator orbits for both protons and neutrons in the valence space [1].

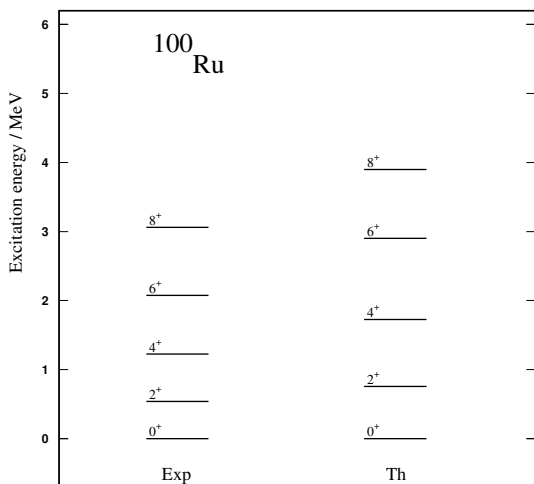


FIG. 1. The theoretical EXVAM spectrum of  $^{100}\text{Ru}$  is compared to the experimental data.

The single particle energies had been adjusted in *complex* Monster(Vampir) calculations for odd mass nuclei in the  $A \simeq 100$  mass region. The effective two-body interaction is constructed from a nuclear matter G-matrix based on the Bonn CD potential. In order to enhance the pairing properties the G-matrix was modified by three short-range (0.707 fm) Gaussians for the isospin  $T = 1$  proton-proton, neutron-neutron, and neutron-proton channels with strengths of -40, -30, and -35 MeV, respectively. The isoscalar spin 0 and 1 particle-particle matrix elements are enhanced by an additional Gaussian with the same range and the strength of -70 MeV. In addition the isoscalar interaction was modified by monopole shifts of -0.275 MeV for all  $T = 0$  matrix elements of the form  $\langle 0g_{9/2}0f; IT = 0 | \hat{G} | 0g_{9/2}0f; IT = 0 \rangle$  involving protons and neutrons occupying the  $0f_{5/2}$  and the  $0f_{7/2}$  orbitals. The Coulomb interaction between the valence protons was added.

### II. 3. Results and Discussion

We investigated the lowest positive parity states up to spin  $8^+$  in  $^{100}\text{Ru}$  including in the Excited Vampir many-nucleon bases up to 14 EXVAM configurations. The final solutions for each spin have been obtained diagonalizing the residual interaction between the considered Excited Vampir configurations.

The theoretical lowest band of  $^{100}\text{Ru}$  is compared to the experimental spectrum in Fig. 1 [2]. The theoretical results on the  $B(E2)$  values for the yrast states presented in Table I compare nicely with experimental data [2].

TABLE I.  $B(E2)$  values (in W.u.) connecting the calculated states (using different effective charges).

Transition	EXVAM	EXVAM
	( $e_p = 1.3, e_n = 0.3$ )	( $e_p = 1.4, e_n = 0.4$ )
$B(E2; 2_1^+ \rightarrow 0_1^+)$	20.5	26.7
$B(E2; 4_1^+ \rightarrow 2_1^+)$	34.2	44.4
$B(E2; 6_1^+ \rightarrow 4_1^+)$	37.5	48.6
$B(E2; 8_1^+ \rightarrow 6_1^+)$	32.4	42.4

[1] A. Petrovici, Phys. Rev. C **85**, 034337 (2012).

[2] T. Konstantinopoulos, A.Petrovici, et al. in preparation

for Phys. Rev. C.